

PREPARATION AND POROUS PROPERTIES OF MATERIALS PREPARED BY SELECTIVE LEACHING OF PHLOGOPITE

KIYOSHI OKADA¹, NORIYUKI NAKAZAWA¹, YOSHIKAZU KAMESHIMA¹, ATSUO YASUMORI¹, JADAMBAA TEMUUJIN^{1,*†}, KENNETH J. D. MACKENZIE² AND MARK E. SMITH³

¹ Department of Metallurgy and Ceramics Science, Graduate School of Science and Engineering, Tokyo Institute of Technology, O-Okayama, Meguro, Tokyo 152-8552, Japan

² The New Zealand Institute for Industrial Research and Development, Lower Hutt, New Zealand

³ Department of Physics, University of Warwick, Coventry, UK

Abstract—Porous silica products obtained by selective leaching of phlogopite using an acid solution were investigated by XRD, MAS NMR, SEM, TEM, DTA/TG, and N₂ and Ar gas adsorptions. The phlogopite powder was leached by a nitric acid solution at various concentrations (0.01–10 M) at 5–150°C for 10 min–480 h. Selective leaching of the phlogopite powder became extensive when the concentration of nitric acid was >1 M. Only SiO₂ remained after the treatment, the other components (MgO, Al₂O₃, K₂O and Fe₂O₃) being selectively leached from the product. At higher leaching temperatures, the leaching rate became faster and the resulting maximum specific surface area of the porous silica product became larger at each leaching temperature. The porous silica products were found by SEM and TEM, to maintain their original platy particle shape even after the selective leaching. The ²⁹Si MAS NMR spectra of the products, however, revealed that the linkage structure of SiO₄ tetrahedra converted to a framework type from a layered type in the original phlogopite. The porous silica product with the maximum specific surface area (532 m²/g) was obtained by leaching in a nitric acid solution with concentration of 5 M at 90°C for 15 min. The pore-size distribution of the porous silica product was bimodal with micropores of ~0.7 nm and mesopores of ~4 nm. The pore size of the products changed from 0.7 nm to 4 nm and further to 6 nm with increased leaching time. The present results are discussed in relation to those reported for phlogopite by other workers.

Key Words—Phlogopite, Porous Properties, Porous Silica, Selective Leaching.

INTRODUCTION

Most clay minerals have a layered structure consisting of SiO₄ tetrahedral sheets and Mg(O,OH)₆, Fe(O,OH)₆ and/or Al(O,OH)₆ octahedral sheets. As there is an apparent difference in strong acid solubility between the Si component and the Mg, Fe and Al components, many procedures have been reported for preparing porous silica by acid treatment of these clay mineral starting materials. As the porous products from these selective leaching methods are expected to show a unique structure, i.e. slit-shape pores compared to a conventionally prepared silica gel, they are considered to have potential as unique adsorbents especially for adsorbing platy molecules. For example, porous silica products have been obtained from 1:1 layered clay minerals such as halloysite (Chon *et al.*, 1978), chrysotile (Le Van Mao *et al.*, 1989; Yasue *et al.*, 1992) and antigorite (Kosuge *et al.*, 1995), and also from 2:1 layered clay minerals such as phlogopite (Harkonen and Keiski, 1984; Kaviratna and Pinnavaia, 1994), hectorite (Kaviratna and Pinnavaia, 1994), sepiolite (Aznar *et al.*, 1996; Myriam *et al.*, 1998; Balci, 1999), palygorskite (Myriam *et al.*, 1998), montmorillonite

(Shinoda *et al.*, 1995), and vermiculite (Suquet *et al.*, 1991). There have been few reports of selective leaching of kaolinite even though it is one of the most widely-used clay minerals in industry, suggesting that it may be difficult to prepare porous products from kaolinite by this method. Two different porous products can be made using kaolinite as the starting material; the kaolinite is converted to metakaolinite before leaching for the preparation of microporous silica (Okada *et al.*, 1998), or it can be calcined to produce a spinel phase and amorphous SiO₂ before selective leaching with alkali for the preparation of mesoporous γ-alumina (Okada *et al.*, 1995).

The porous properties such as specific surface area (S_{BET}) of these reported porous products vary considerably, from ~20 to 620 m²/g. The characteristics of the porous silica products are generally similar to those of conventional SiO₂ gel with a three-dimensional framework structure. However, some porous silica products obtained from 1:1 layered clay minerals such as antigorite (Kosuge *et al.*, 1995) and metakaolinite (Okada *et al.*, 1998) are reported to retain their layered structure, the slit-shaped pores being considered to form between the layers. The wide variety of S_{BET} values in these porous silica products is, of course, caused by the differences in the chemical composition, and structure of the starting materials, and also by variations in the leaching conditions, *i.e.* the nature and concentration of

* E-mail address of corresponding author:

kokada@ceram.titech.ac.jp

† Permanent address: The Institute of Chemistry and Chemical Technology, Mongolian Academy of Sciences, Ulaanbaatar 51, Mongolia

leachate, the solid/solution ratio, temperature, time, etc. The value of S_{BET} reported in phlogopite by Kaviratna and Pinnavaia (1994) was $20\text{ m}^2/\text{g}$ whereas that found by Harkonen and Keiski (1984) was very different ($620\text{ m}^2/\text{g}$). The reason for this discrepancy is unclear. The structure of the porous silica products was not well characterized in those papers.

We are interested in the porous silica obtained from phlogopite for the following reasons: (1) the reported S_{BET} is amongst the largest of the porous silicas produced by selective leaching of clay minerals; (2) there are major discrepancies in the previously reported S_{BET} values as mentioned above; (3) we believe there is a possibility of developing porous products with acidic properties arising from the presence of AlO_4 incorporated in the SiO_4 tetrahedral sheets of the original phlogopite; and (4) a large amount of phlogopite powder is commercially available which could be used as an industrial starting material for the production of porous silica if the products were found to have useful properties.

In the present work, phlogopite powder was leached with nitric acid solution in various concentrations, for various temperatures and times. The chemical compositions of the products were examined by X-ray fluorescence (XRF) and their porous properties, structures and solid acidity were characterized using gas adsorption, powder X-ray diffraction (XRD), differential thermal analysis-thermal gravimetry (DTA-TG), scanning electron microscopy (SEM), transmission electron microscopy (TEM) and solid-state ^{29}Si and ^{27}Al magic angle spinning (MAS) nuclear magnetic resonance (NMR).

EXPERIMENTAL METHODS

Preparation

Phlogopite from Suzor, Lac Letondal, Quebec, Canada, was used as the starting material. The commercially available mineral (200-HK, Suzorite® mica, Marietta Resources International) had an average flake size of $90\text{ }\mu\text{m}$, according to the supplier's specifications.

In the initial leaching experiments, the powder samples were treated in nitric acid solutions at various concentrations from 10^{-2} to 5 M to determine the optimum acid concentration. The experiments were carried out at 150°C using an autoclave to speed up the reaction. Selective leaching was carried out by stirring in 100 mL of 5 M nitric acid with 2 g of the powder at temperatures of $5, 10, 30, 60$ and 90°C for various times from 15 min to 480 h . The leaching experiments at 5 and 10°C were performed in a refrigerator whereas a heated stirrer was used for those at $30, 60$ and 90°C . A Pyrex glass reaction flask equipped with a reflux condenser was used to avoid evaporation of the solution during the experiments. After leaching, the product was washed once with dilute nitric acid (0.5 M), followed by three washings with distilled water, filtered and dried at 110°C overnight.

Characterization

X-ray diffraction patterns were recorded on a Rigaku Geigerflex diffractometer with monochromated $\text{CuK}\alpha$ radiation. The chemical compositions were determined by XRF using a Rigaku RIX2000 spectrometer. The DTA/TG curves were recorded up to 1250°C at a heating rate of $10^\circ\text{C}/\text{min}$ in a dynamic atmosphere of dry air using a Rigaku Thermoplus TG8120 instrument. The microstructure of the samples was observed by SEM using a JEOL JSM-5310 electron microscope at an accelerating voltage of $10, 15$ or 20 kV and also by TEM using an Hitachi S-9000 electron microscope at 300 kV . Solid-state ^{29}Si MAS NMR spectra were obtained at 7 T using a Bruker spectrometer and Doty probe spun at 3.5 kHz . The ^{29}Si spectra were acquired using a 30° pulse of $2\text{ }\mu\text{s}$ and a recycle time of 4 s , and were referenced to tetramethylsilane (TMS). The ^{27}Al spectra were acquired at 14.1 T using a Chemagnetics Infinity 600 spectrometer with a 3.2 nm probe spun at 18 kHz . A 15° pulse of $0.5\text{ }\mu\text{s}$ and a recycle time of 1 s , was used and the spectra were referenced to the secondary standard of the AlO_6 resonance of $\text{Y}_3\text{Al}_5\text{O}_{12}$ at 0.7 ppm .

Porous properties

Nitrogen gas adsorption-desorption isotherms were measured using a Quantachrome Autosorb-1 instrument at 77 K . The measurements were made after degassing under vacuum at 200°C for 5 h . The specific surface area (S_{BET}) was calculated by the BET method (Brunauer *et al.*, 1938) and pore-size distribution was calculated by the BJH method (Barrett *et al.*, 1951) using the desorption isotherms. The total pore volume was calculated from the maximum amount of nitrogen gas adsorption at partial pressure (P/P_0) = 0.999 . For micropore analysis, Ar gas adsorption isotherms were measured using a Quantachrome Autosorb-1 instrument at 87.5 K . The pore-size distribution of the micropores was calculated by the HK method (Horvath and Kawazoe, 1983) applicable to slit-shaped pores.

RESULTS AND DISCUSSION

Starting material

The as-received phlogopite powder was characterized by XRF, XRD, DTA/TG and N_2 gas adsorption. As shown in Figure 1, the sample contained a small amount of chlorite and an unknown phase as accessory minerals. The chemical composition analyzed by XRF is listed in Table 1 (on a dry weight basis). The chemical formula of the phlogopite calculated from Table 1, ignoring the influence of the accessory minerals, is $\text{K}_{0.79}[\text{Mg}_{2.58}\text{Fe}_{0.27}\text{Al}_{0.13}][\text{Si}_{2.97}\text{Al}_{0.99}]\text{O}_{10}(\text{OH},\text{F})_2$. As shown in Figure 2, the TG curve indicates a two-step weight loss, with steps at ~ 600 and 1000°C . The loss on ignition observed up to 1000°C is 2.5 mass\% , with a second loss above 1000°C of 5.6 mass\% , the total loss up

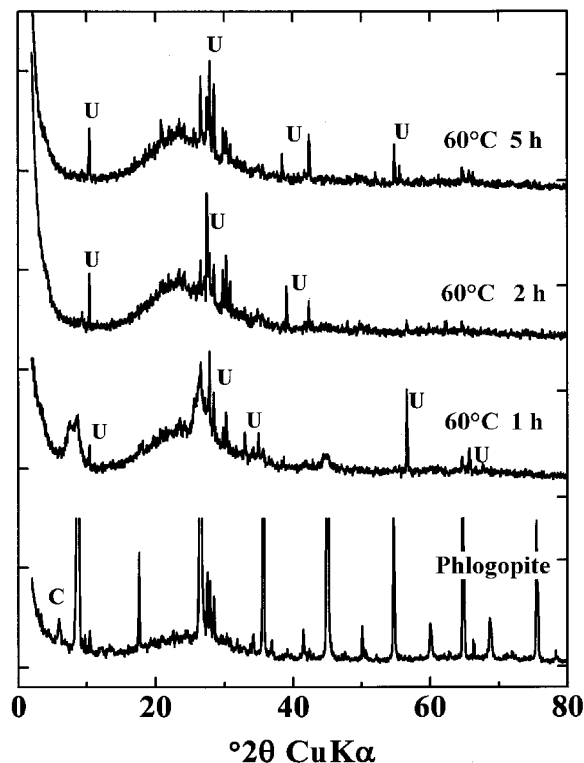


Figure 1. XRD patterns of phlogopite and porous products leached by 5 M HNO_3 at 60°C for 1, 2 and 5 h. Unmarked peaks: phlogopite, C: chlorite, U: unknown phase.

Table 1. Chemical composition as measured by XRF and porous properties of samples as measured by BET using N_2 gas as the adsorbate.

Sample	Preparation condition			Chemical composition (atm.%)					Porous property*		
	Conc. (M)	Temp. (°C)	Time (h)	Si	Al	Mg	Fe	K	S_{BET} ($\text{m}^2 \text{g}^{-1}$)	V_p (mL g^{-1})	D_p (nm)
As-received	—	—	—	38.4	14.5	33.4	3.5	10.2	2	0.01	—
5N5-7D	5	5	168	76.6	5.5	12.9	1.9	3.1	260	0.36	5.6
5N5-8D	5	5	192	89.2	2.8	5.4	1.1	1.5	—	—	—
5N5-10D	5	5	240	86.4	3.5	7.0	1.2	1.9	262	0.42	7.8
5N5-12D	5	5	288	93.3	2.0	2.8	0.8	1.2	241	0.52	8.0
5N5-20D	5	5	480	93.7	1.9	2.7	0.7	1.0	220	0.48	11.0
5N10-4D	5	10	96	85.1	3.9	7.4	1.3	2.2	—	—	—
5N10-6D	5	10	144	92.9	2.1	3.2	0.7	1.0	—	—	—
5N10-7D	5	10	168	92.5	2.7	3.0	0.7	1.2	—	—	—
5N30-5H	5	30	5	55.4	10.3	25.8	3.1	5.4	—	—	—
5N30-15H	5	30	15	86.4	3.5	6.8	1.3	2.0	352	0.40	3.6
5N30-20H	5	30	20	92.6	2.2	3.2	0.8	1.1	356	0.41	4.2
5N30-25H	5	30	25	93.3	2.0	3.0	0.8	1.0	357	0.43	4.6
5N60-1H	5	60	1	79.4	4.5	9.2	2.9	4.0	233	0.28	3.2>1.8
5N60-2H	5	60	2	95.2	1.4	2.0	0.6	0.8	418	0.35	3.2>2.2
5N60-5H	5	60	5	95.4	1.4	1.8	0.7	0.8	383	0.39	3.6
5N60-10H	5	60	10	93.9	1.8	2.5	0.7	1.1	331	0.39	4.6>3.8
5N90-10M	5	90	1/6	86.9	3.2	6.7	1.2	2.0	471	0.32	0.7>3.0
5N90-15M	5	90	1/4	93.3	2.0	2.9	0.8	1.1	532	0.36	0.7>3.0
5N90-20M	5	90	1/3	93.7	1.9	2.7	0.7	1.0	527	0.39	0.7>3.0
5N90-30M	5	90	1/2	93.4	2.0	2.8	0.7	1.1	527	0.42	0.7>3.2
5N90-1H	5	90	1	93.9	1.8	2.6	0.7	1.0	458	0.36	3.6
5N90-5H	5	90	5	96.2	1.7	2.1	0.0	0.0	271	0.35	3.6>5.4

* S_{BET} : specific surface area; V_p : total pore volume; D_p : pore diameter

to 1250°C being 8.1 mass%. If we assume the first loss represents evaporation of OH and the second loss that of F, the atomic ratio of OH/F in the phlogopite is 33/67. The calculated weight loss of the phlogopite based on this composition is 7.5 mass%, in fair agreement with the observed ignition loss of 8.1 mass%. The measured S_{BET} of this powder was 2 m^2/g .

Result of selective leaching

Figure 3 shows the chemical composition of the phlogopite before and after leaching at 150°C as a function of concentration of the nitric acid solution. Over the concentration range 10^{-2} to 2×10^{-1} M the chemical composition changed little even on accelerated leaching at elevated temperature. A slight loss of K_2O was observed, as was a slight increase of Fe_2O_3 due to relative condensation. At concentrations of 2×10^{-1} to 1 M, an apparent increase of SiO_2 and a decrease of all the other components was observed. The chemical compositions of the products were changed drastically by leaching at concentrations >2 M. Only the SiO_2 content was increased by the leaching treatment but all the other components (MgO , Al_2O_3 , Fe_2O_3 and K_2O) decreased markedly. It is therefore preferable to use relatively concentrated nitric acid to selectively leach phlogopite in a reasonable time. We chose 5 M for the subsequent leaching experiments.

Leaching experiments were carried out in 5 M nitric acid solution at temperatures from 5 to 90°C for various

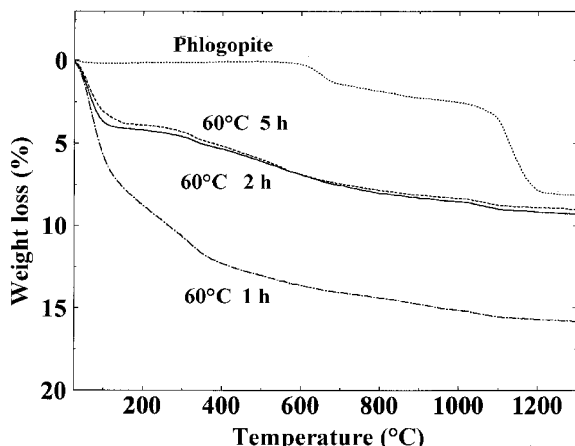


Figure 2. TG curves of phlogopite and porous products leached by 5 M HNO_3 at 60°C for 1, 2 and 5 h.

times. The chemical compositions of the products are listed in Table 1. Changes of the major components SiO_2 and MgO in the products as measured by XRF are plotted for each leaching temperature as a function of leaching time in Figure 4. At each temperature, the SiO_2 content increased with longer leaching time and became almost constant at ~93 atm.%. On the other hand, the MgO concentration decreased to a constant level of ~2–3 atm.%. The leaching time required to achieve steady-state equilibrium decreased with increasing temperature.

Porous properties

The S_{BET} of the products prepared by leaching at various temperatures and times are listed in Table 1. Changes in the S_{BET} of the products prepared at several leaching temperatures are shown in Figure 5 as a function of leaching time. The maximum S_{BET} obtained at each leaching temperature varied greatly, ranging from 262 m^2/g at 5°C to 532 m^2/g at 90°C. There is a clear tendency to higher maximum S_{BET} values with higher leaching temperature. This result indicates that faster leaching conditions give products with higher S_{BET} values, and this is suggested to correspond to the resultant pore sizes as listed in Table 1.

The pore-size distributions (PSD) of the products leached at 60 and 90°C for various times are shown in Figures 6 and 7, respectively. At 90°C, the PSD became gradually narrower with increasing leaching time up to 5 h and became bimodal after leaching for 10 h (Figure 6). Thus, the pore size (pore diameter and not radius) was found to increase with leaching time from 3.4 nm after leaching for 2 h to 3.8 nm at 5 h and further to 5 nm at 10 h. The increase in pore size is related to the decrease of S_{BET} with prolonged leaching. In these porous products, the resulting pore size was much larger than that expected to evolve by selective leaching of the octahedral sheets, which is calculated from crystal structure to be ~0.3 nm. (A small increase observed in

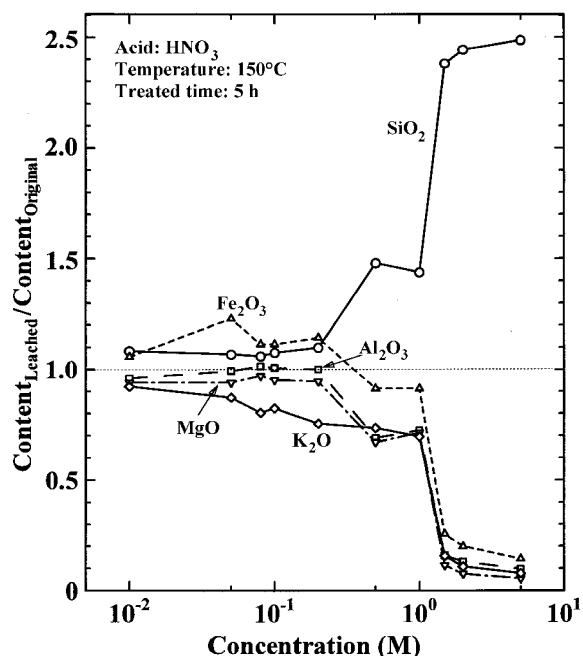


Figure 3. Change of ratio of each component before and after leaching, as a function of concentration of nitric acid solution.

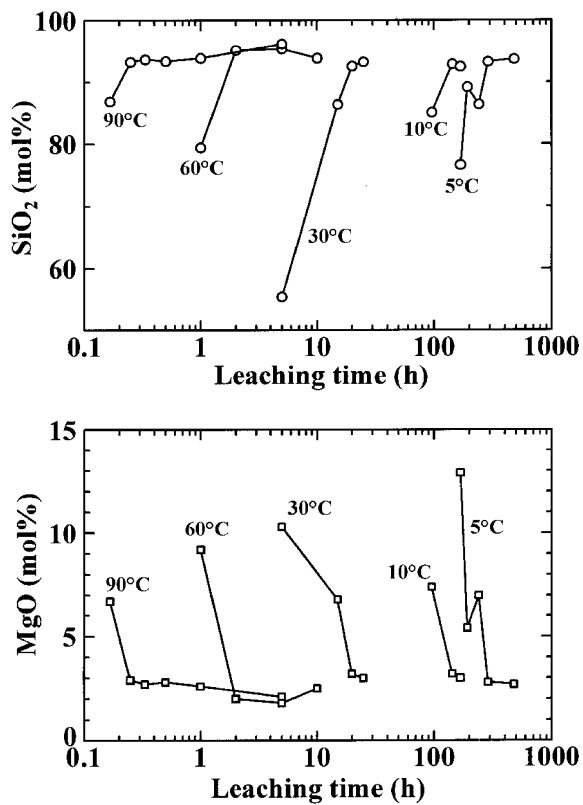


Figure 4. Changes of SiO_2 and MgO content in porous products as a function of leaching time, as measured by XRF.

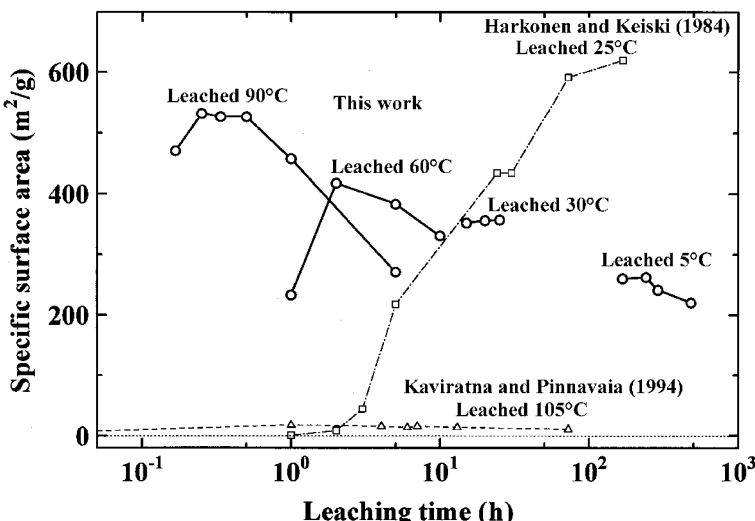


Figure 5. Changes of specific surface areas of porous products leached by 5 M HNO₃ at various temperatures as a function of leaching time.

the PSD in the micropore range (≤ 2 nm pore size) for these products was small compared with the peak height of the mesopores (2–50 nm pore size).

On the other hand, the PSDs of the porous products leached at 90°C showed a greater increase of peak area in micropore range and a lower peak at 3.4 nm compared with the porous products leached at 60°C. The micropores in these products were therefore analyzed using the HK method. Figure 8 shows the PSDs of the porous products leached at 90°C for various times. In these PSDs, a peak was observed at a pore width of ~ 0.7 nm, corresponding to approximately twice the pore size calculated geometrically. Since the peak height of the micropores decreased and that of the mesopores increased with increased leaching time, the micropores formed by selective leaching of the octahedral sheets of

the phlogopite structure are suggested to be rather unstable, with mesopores of ~ 3 –4 nm in diameter developing almost simultaneously by further structural rearrangement during prolonged selective leaching. As described previously, the sizes of the mesopores increase further with longer leaching times. This is considered to be caused by excess leaching of the porous structure. That is, selective leaching of Mg, Fe, Al and K cations begins at phlogopite surfaces resulting in the formation of micropores. The surface micropores are not stable to further leaching however, and enlarge to mesopores. Simultaneously, micropore formation continues deeper in the surface layer structure. (Pore formation proceeds into the interior of the phlogopite particles with the pore size changing from micropores to mesopores and increasing in size from the inside to the surface with

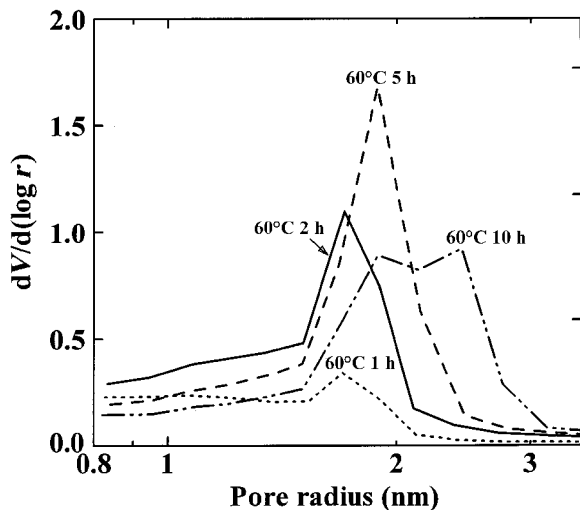


Figure 6. Pore-size distributions of porous products leached by 5 M HNO₃ at 60°C for various times.

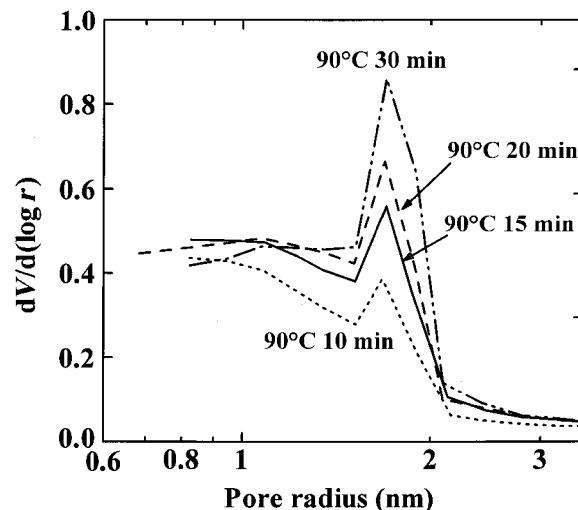


Figure 7. Pore-size distributions of porous products leached by 5 M HNO₃ at 90°C for various times.

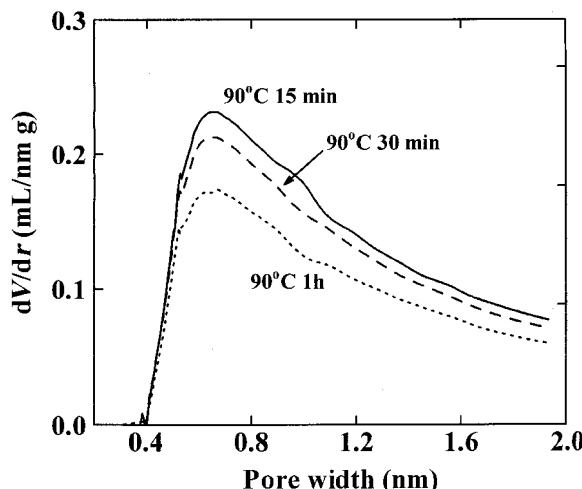


Figure 8. Micropore-size distributions of porous products leached by 5 M HNO₃ at 90°C for various times calculated by the HK method.

longer leaching times.) The particle size is therefore considered to be an important factor in enhancing the porous properties of the leached products of phlogopite.

The pore-size change with leaching time in the present products is very different from that reported for metakaolinite (Okada *et al.*, 1998) because it formed only micropores with constant pore size (0.6 nm) and no mesopores, even those treated for a prolonged period of time. This may be due to the difference in the residual SiO₄ tetrahedra in the 2:1 and 1:1 layered structures. In the 2:1 structure, the apical silanol groups of the SiO₄ tetrahedral sheets formed by selective leaching of the Mg octahedral sheets face each other, and may readily condense to form a framework structure. Furthermore, leaching of the AlO₄ tetrahedra substituted for SiO₄ tetrahedra in the phlogopite may help to enhance rearrangement of the residual layered structure in the product to form framework structure. On the other hand, the apical silanol groups, formed by selective leaching of the Al octahedral sheets in a 1:1 layered structure face the same direction, thereby suppressing condensation in the products formed from metakaolinite (Okada *et al.*, 1998) and resulting in pore sizes which change little even after prolonged leaching.

Characterization of porous products

Figure 9 shows the microstructure of the phlogopite powder and porous products leached at 60°C for various times as imaged with SEM. Although the particle sizes are seen to become slightly smaller during leaching, the layered particle shape is retained even after prolonged leaching treatment. As shown in Table 1, the chemical compositions of the porous products are converted almost completely to SiO₂ (90%) after prolonged leaching treatment. X-ray diffraction (Figure 1) indicates that the structure of the porous products is amorphous though some peaks of an unknown phase

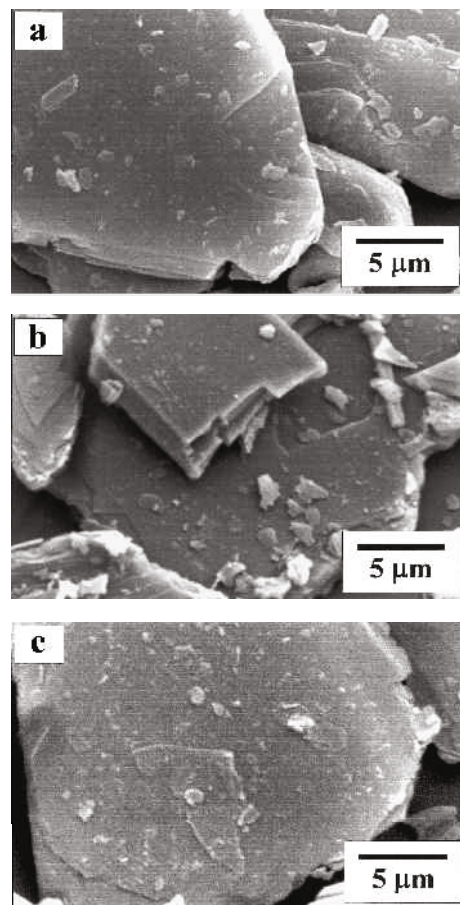


Figure 9. SEM images of as-received phlogopite (a) and porous products leached by 5 M HNO₃ at 60°C for 15 min (b) and 5 h (c).

are observed. Several total atm.% of Al, Mg, Fe and K cations residue in the 5N60-5H may correspond to the unknown phase. This phase may, however, have only a little influence in reducing the real S_{BET} of the porous silica product. The TG curves of the porous products (Figure 2) show a steep weight loss up to 100°C, which we attribute to desorption of physisorbed water molecules, and gradual weight loss above 300°C, which we attribute to condensation of the silanol Si-OH groups and subsequent evaporation of water. Of the three leached products, that leached for 1 h showed a greater weight loss than the others. Since this material also showed a rather lower S_{BET} than the other products, it appears to be unusual, but the reasons for this are unclear.

The local environments of the Si and Al atoms in the porous products were examined by MAS NMR. Figures 10 and 11 show the ²⁹Si and ²⁷Al MAS NMR spectra of the porous products leached at 60°C for various times. The ²⁹Si MAS NMR spectra show two overlapping peaks at -111 and -102 ppm with a shoulder at ~ -93 ppm. The -111 ppm peak is assigned to the Q⁴ structural unit, corresponding to a three-

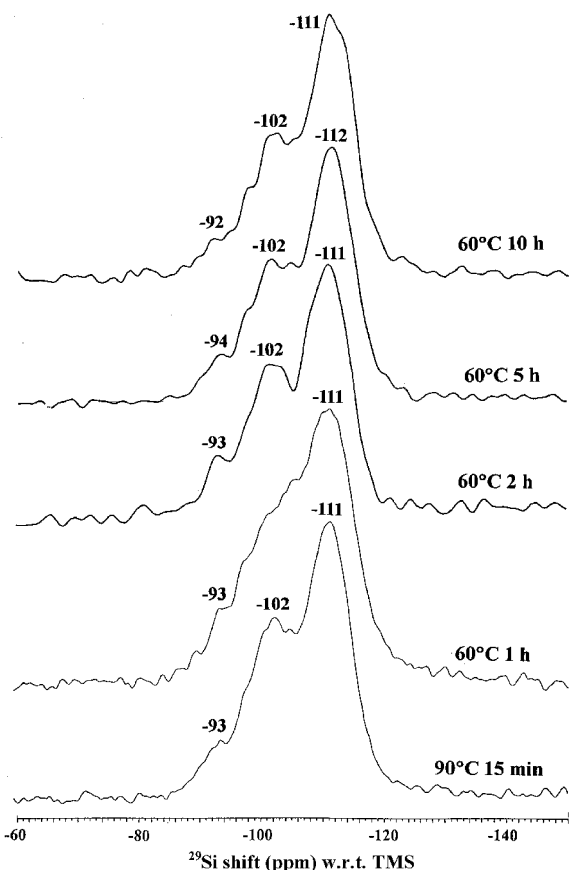


Figure 10. ^{29}Si MAS NMR spectra of porous products leached by 5 M HNO_3 at 60°C for various times and 90°C for 15 min.

dimensional framework structure while the -102 ppm peak may be assigned to the Q^3 structural unit corresponding to a layered structure; alternatively, it could be assigned to a three-dimensional framework structure with a non-bridging oxygen site, *i.e.* one silanol group. The Q^4 peak intensity was much larger than that of Q^3 in these products. These spectra are rather different from that reported by Kaviratna and Pinnavaia (1994), whose reported spectrum of their leached phlogopite showed a distinct Q^4 peak (-111.6 ppm) with only a tail at about the Q^3 peak position (-103 ppm). The Q^3/Q^4 peak intensity ratios of the silica products prepared from various clay minerals are listed in Table 2; the Q^3/Q^4 ratio of the present product is apparently greater than that reported by Kaviratna and Pinnavaia (1994). The present result is compatible with the data reported for the products from the 2:1 layered structures such as hectorite and sepiolite. It is different, however, from those reported for the porous silica products from the layered structures metakaolinite (Okada *et al.*, 1998) and antigorite (Kosuge *et al.*, 1995) which showed a much larger Q^3/Q^4 ratio than the present porous silica products. The porous silica products with greater Q^3/Q^4 ratios were

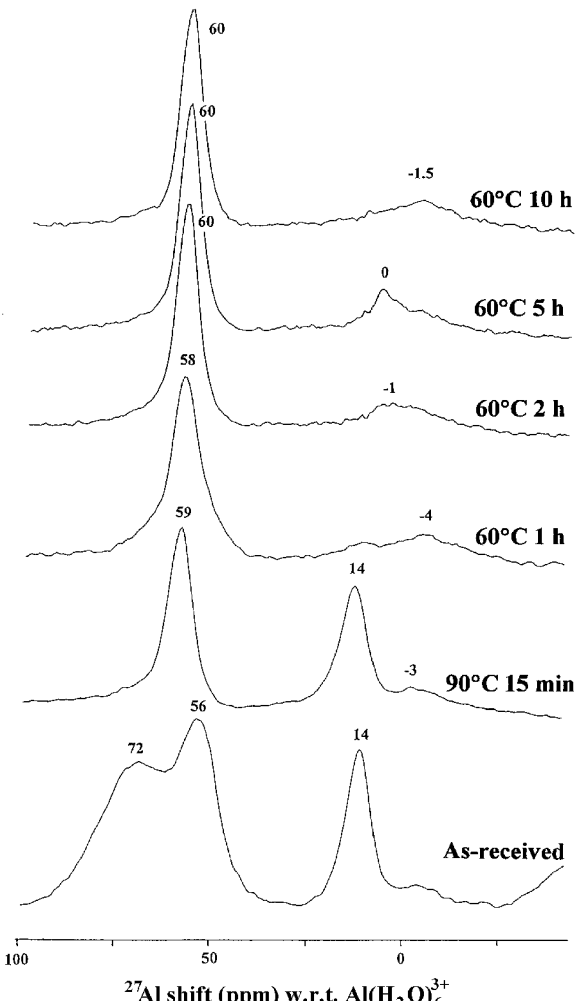


Figure 11. ^{27}Al MAS NMR spectra of phlogopite and porous products leached by 5 M HNO_3 at 60°C for various times and 90°C for 15 min.

microporous and the pores were found to be formed in the layered structure. On the other hand, the mean pore size of the silica products from sepiolite, which shows similar Q^3/Q^4 ratios to the present products was reported to be in the range 6–12 nm by Aznar *et al.* (1996). From these results, and based on the PSD of the present products, the porous silica structure is suggested to consist of a layered part which forms micropores and a framework part which forms mesopores. Since the ^{27}Al MAS NMR spectra of the products show a peak at ~60 ppm assigned to tetrahedral coordination (Figure 11), some of the Q^3 peak may contain a contribution from the $\text{Q}^4(1\text{Al})$ structural unit.

Transmission electron micrographs of phlogopite and its porous silica product (5N60-5H) are shown in Figure 12. The micrograph of the product shows little change compared with a platy particle shape of the original phlogopite. The selected area electron diffraction of the original phlogopite shows a spotty hexagonal

Table 2. Q^3/Q^4 ratios of ^{29}Si MAS NMR spectra of silica products from various clay minerals.

Starting material	Layer type	Q^3/Q^4 ratio*	Reference
Phlogopite	2:1	0.57	This study
Phlogopite	2:1	0.17	Kaviratna and Pinnavaia (1994)
Fluorohectorite	2:1	0.23	Kaviratna and Pinnavaia (1994)
Hectorite	2:1	0.50	Komadel <i>et al.</i> (1996)
Sepiolite	2:1	0.61	Aznar <i>et al.</i> (1996)
Kaolinite	1:1	0.85	Okada <i>et al.</i> (1998)
Antigorite	1:1	0.71	Kosuge <i>et al.</i> (1995)

* Peak intensity ratio of Q^3 (-102 ppm)/ Q^4 (-111 ppm)

pattern corresponding to the $hk0$ plane as in Figure 12a while that of the product shows an amorphous halo pattern as in Figure 12b. Thus, the product retains pseudomorphic platy shape after conversion to porous silica.

Comparison of porous properties

As shown in Figure 5, the relationship between S_{BET} and leaching time determined in this work is very different from that of phlogopite reported by Harkonen and Keiski (1984) and by Kaviratna and Pinnavaia (1994). Harkonen and Keiski (1984) reported an increase of S_{BET} with increased leaching time at 25°C. The maximum S_{BET} value of 620 m²/g was obtained after leaching for 168 h. By contrast, we did not obtain as large an S_{BET} value by leaching at 30°C, a similar temperature to that of Harkonen and Keiski (1984). The maximum S_{BET} value obtained at this temperature was ~360 m²/g, much lower than that of Harkonen and Keiski (1984). Much greater S_{BET} values could only be obtained by leaching at higher temperatures. The PSDs of our porous products are quite similar to those reported by Harkonen and Keiski (1984), *i.e.* mesopores with a relatively narrow peak at ~3–4 nm and micropores with broad profile at ~2 nm or less. The difference in the S_{BET} values (620 and 360 m²/g) is therefore attributed to the numbers of micropores and mesopores in the products. The porous products reported by Harkonen and Keiski

(1984) contain more micropores than the products in the present study. This may arise from differences in the particle size and chemical composition of phlogopites used as the starting materials because it is expected that these factors have a great influence on selective leaching. The particle size of the present phlogopite was much smaller than that used by Harkonen and Keiski (1984), ruling this out as a factor for the difference in S_{BET} . The chemical composition of the phlogopite is likely to be of greater importance, especially the amount of substitution of Al and/or Fe for Si in the tetrahedral sheets, as leaching of AlO_4 and/or FeO_4 tetrahedra should facilitate the structural rearrangement of the residual layered structure leading to the loss of micropores. Although the total amount of substitution of Al and/or Fe for Si in the tetrahedral sheets should ideally be constant in phlogopite, differences may occur in the ratio of Al/Fe from sample to sample. The concentration of Fe^{3+} in phlogopite may therefore affect the porous properties of the products, as Al is more soluble than Fe^{3+} in acid solution (Loughnan, 1969). Although Harkonen and Keiski (1984) did not report the chemical composition of the phlogopite they used, their sample contained a relatively high proportion of Fe (Fe/Mg ratio of 0.19). This Fe/Mg ratio is much higher than that of the phlogopite used in this study (Fe/Mg = 0.10) as well as that used by Kaviratna and

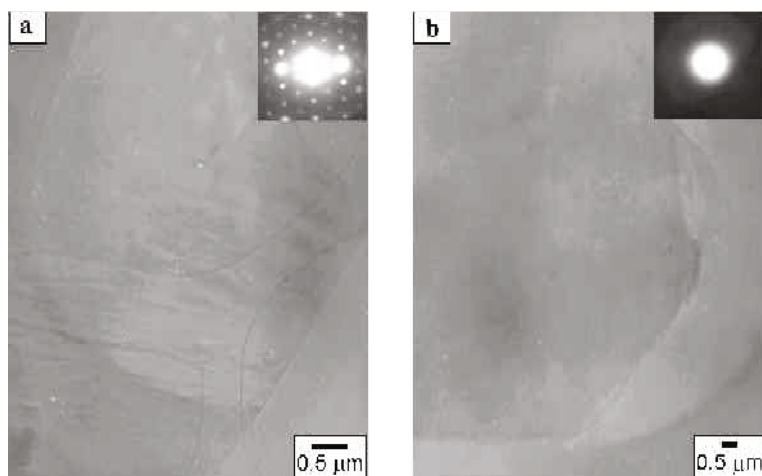


Figure 12. TEM images of phlogopite (a) and porous product leached by 5 M HNO_3 at 60°C for 5 h (b).

Pinnavaia (1994) ($\text{Fe}/\text{Mg} = 0$). This factor may be one of the reasons for the different S_{BET} values of the porous products from the three different phlogopites.

Compared with the high S_{BET} value ($>500 \text{ m}^2/\text{g}$) reported in the present paper and also by Harkonen and Keiski (1984), Kaviratna and Pinnavaia (1994) observed a very low S_{BET} value for their product obtained by selective leaching of phlogopite at 105°C . As their leaching was carried out at 105°C , the present leaching experiments at 90°C may be compared with their results. Although their leaching temperature was higher than the present temperature, using the same acid concentration, their leaching rate of Mg was very sluggish; only 50% of Mg was leached after 1 h at 105°C (Kaviratna and Pinnavaia, 1994) compared with 80% of Mg leached after 10 min at 90°C in the present study. Because they did not mention whether their leaching treatment was carried out with stirring, we cannot determine the discrepancy. One important factor may be the ratio of acid to phlogopite ($\text{H}/\text{Mg} = 5$ (Kaviratna and Pinnavaia, 1994), compared with 40 (present work)). Unfortunately Harkonen and Keiski (1984) did not report their acid/phlogopite ratio. As mentioned above, faster leaching increases the S_{BET} value of the product because the micropores originally formed by selective leaching of octahedral sheets of phlogopite are rapidly changed into mesopores, further increasing in size and reducing the S_{BET} value. Higher leaching temperatures may also promote the rearrangement reaction to condense SiO_4 tetrahedra, reducing the S_{BET} of the products.

CONCLUSIONS

The products of phlogopite powder selectively leached in nitric acid at various concentrations, temperatures and times were amorphous SiO_2 with a Q^4 framework and Q^3 layered structures ($\text{Q}^4 > \text{Q}^3$). The specific surface area of the products increased with higher leaching temperatures. The pore size changed from 0.7 nm micropores to 3–4 nm mesopores which became >4 nm at longer leaching times. The size of the micropores was in good agreement with the value calculated geometrically assuming selective leaching of the octahedral sheets of the starting phlogopite. The maximum specific surface area achieved was $532 \text{ m}^2/\text{g}$, with a total pore volume of 0.52 mL/g .

ACKNOWLEDGMENTS

JT thanks the Japan Society for Promotion of Science for the award of a research fellowship under which this work was carried out.

REFERENCES

- Aznar, A.J., Gutierrez, E., Diaz, P., Alvarez, A. and Poncelet, G. (1996) Silica from sepiolite: Preparation, textural properties, and use as support to catalysts. *Microporous Materials*, **6**, 105–114.
- Balci, S. (1999) Effect of heating and acid pre-treatment on pore size distribution of sepiolite. *Clay Minerals*, **34**, 647–655.
- Barrett, E.P., Joyner, L.G. and Halenda, P.P. (1951) The determination of pore volume and area distributions in porous substances. I. Computations from nitrogen isotherms. *Journal of the American Chemical Society*, **73**, 373–380.
- Brunauer, S., Emmet, P.H. and Teller, E. (1938) Adsorption of gases in multimolecular layers. *Journal of the American Chemical Society*, **60**, 309–319.
- Chon, M.C., Tsuru, T. and Takahashi, H. (1978) Changes in pore structure of kaolin mineral by sulfuric acid treatment. *Clay Science*, **5**, 155–162.
- Harkonen, M.A. and Keiski, R.L. (1984) Porosity and surface area of acid-leached phlogopite: The effect of leaching conditions and thermal treatment. *Colloids and Surfaces*, **11**, 323–339.
- Kaviratna, H. and Pinnavaia, T.J. (1994) Acid hydrolysis of octahedral Mg^{2+} sites in 2:1 layered silicates: An assessment of edge attack and gallery access mechanisms. *Clays and Clay Minerals*, **42**, 717–723.
- Komadel, P., Madejová, J., Janek, M., Gates, W.P., Kirkpatrick, R.J. and Stucki, J.W. (1996) Dissolution of hectorite in inorganic acids. *Clays and Clay Minerals*, **44**, 228–236.
- Kosuge, K., Shimada, K. and Tsunashima, A. (1995) Micropore formation by acid treatment of antigorite. *Chemistry Materials*, **7**, 2241–2246.
- Le Van Mao, R., Kipkemboi, P., Levesque, P., Vailancourt, A. and Denes, G. (1989) Leached asbestos materials: Precursors of zeolites. *Zeolites*, **9**, 405–411.
- Loughnan, F.C. (1969) *Chemical Weathering of the Silicate Minerals*. Elsevier, New York, 154 pp.
- Myriam, M., Suarez, M. and Martin-Pozas, J.M. (1998) Structural and textural modifications of palygorskite and sepiolite under acid treatment. *Clays and Clay Minerals*, **46**, 225–231.
- Okada, K., Shimai, A., Takei, T., Hayashi, S., Yasumori, A. and MacKenzie, K.J.D. (1998) Preparation of microporous silica from metakaolinite by selective leaching method. *Microporous and Mesoporous Materials*, **21**, 289–296.
- Shinoda, T., Onaka, M. and Izumi, Y. (1995) Proposed models of mesopore structures in sulfuric acid-treated montmorillonites and K10. *Chemistry Letters*, **1995**, 495–496.
- Suquet, H., Chevalier, S., Marcilly, C. and Barthomeuf, D. (1991) Preparation of porous materials by chemical activation of the Llano vermiculite. *Clay Minerals*, **26**, 49–60.
- Yasue, T., Kojima, Y. and Arai, Y. (1992) Recent study of and problems with surface improvement of asbestos. *Gypsum and Lime*, **238**, 194–204 (in Japanese).

(Received 13 November 2001; revised 15 March 2002; Ms. 602; A.E. Peter J. Heaney)